

Journal of Materials Chemistry A

Accepted Manuscript



This is an *Accepted Manuscript*, which has been through the Royal Society of Chemistry peer review process and has been accepted for publication.

Accepted Manuscripts are published online shortly after acceptance, before technical editing, formatting and proof reading. Using this free service, authors can make their results available to the community, in citable form, before we publish the edited article. We will replace this *Accepted Manuscript* with the edited and formatted *Advance Article* as soon as it is available.

You can find more information about *Accepted Manuscripts* in the [Information for Authors](#).

Please note that technical editing may introduce minor changes to the text and/or graphics, which may alter content. The journal's standard [Terms & Conditions](#) and the [Ethical guidelines](#) still apply. In no event shall the Royal Society of Chemistry be held responsible for any errors or omissions in this *Accepted Manuscript* or any consequences arising from the use of any information it contains.

Cite this: DOI: 10.1039/c0xx00000x

Full paper

www.rsc.org/xxxxxx

A fast room-temperature strategy for direct reduction of graphene oxide films towards flexible transparent conductive films

Jing Ning,^{a,b#} Jie Wang,^{a#} Xianglong Li,^a Tengfei Qiu,^{a,b} Bin Luo,^a Long Hao,^{a,b} Minghui Liang,^a Bin Wang,^{a,b} and Linjie Zhi^{*a}

Received (in XXX, XXX) Xth XXXXXXXXX 20XX, Accepted Xth XXXXXXXXX 20XX

DOI: 10.1039/b000000x

Chemically reduced graphene oxide (rGO) is widely studied as transparent electrodes, as it can be cheaply prepared on a large scale, easily integrated into flexible devices, and contributes to excellent device performances. However, the commonly used reduction methods to converting graphene oxide (GO) films into rGO ones generally involve toxic reagents or complex transfer steps. In this report, we develop a simple short-term room-temperature strategy for the direct fabrication of rGO-based transparent conductive films on flexible substrates, where tin (Sn) is used to promote the conversion of pre-deposited GO films into rGO ones. The thus-prepared rGO films exhibit sheet resistances of 6.7–17.3 k Ω sq⁻¹ and transparencies of 75–81% at 550 nm, indicating great potential of the here-developed methodology for the fabrication of graphene-based transparent conductive films, at conditions without any heating and transferring processes, as well as toxic agents.

Introduction

Transparent conductive films (TCFs) are indispensable in a variety of optoelectronic devices, including solar cells,^{1,2} touch panels,³ liquid-crystal displays (LCDs) and light emitting diodes (LEDs).⁴ Currently, indium tin oxide (ITO) is the most commonly used material commercially available in the market. Admitting that ITO shows excellent transparency and conductivity, there are still critical problems remain unsolved, such as the limited indium source on earth, the high cost, the fragility of the film that comes from the inorganic nature.⁵ Therefore, to find out alternatives for ITO, especially materials for flexible devices, is urgently required.

Since its discovery in 2004, graphene, with its unique two-dimensional structure, has raised the attention of scientists from a lot of research fields,⁶ covering electronics and optoelectronics,⁷ sensors,⁸ energy storage devices,^{9,10} and so on. Given its high room-temperature conductivity, excellent transmittance and outstanding flexibility, graphene is considered as an ideal material for TCFs as well.^{5,11} A number of methods have been developed to fabricate graphene based TCFs, among which, chemical reduction of graphene oxide (GO) is known as a reliable route for mass production of graphene thin films,¹² especially on flexible substrates.^{13–17} As the reduced graphene oxide (rGO) is difficult to be well dispersed, solution-based approaches for the scalable fabrication of thin films, like Mayer-rod coating, spray coating, dip coating, spin-coating, and Langmuir-Blodgett method are quite limited.^{18–20} Consequently, it is preferred that a GO thin film is firstly formed on the target substrate, and then

followed by a reducing process. Accordingly, directly reducing GO in the film modality is significantly important. Some reducing agents, such as hydrazine^{21,22} and hydriodic acid^{13,14,23} have been successfully used to reduce GO film. However, the use of these toxic chemicals agents can result in serious environmental problems especially when used on a large scale.

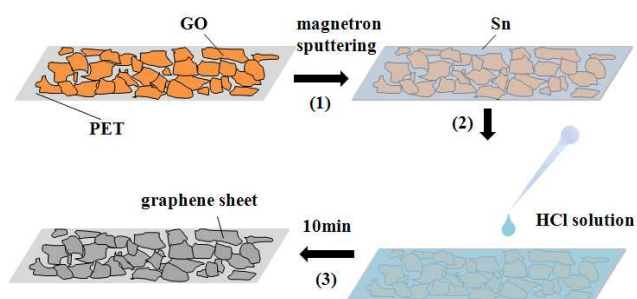
Some non-noble metals (e.g., Fe, Zn, Al, Sn) are well known to act as eco-friendly reducing agents in many reaction. Very recently these reducing metals have been successfully employed to reduce GO as well.^{24–29} In most cases, the involved reactions are conducted either in a hot solution, or upon heating, or for a long period of time, which are disadvantageous for further integration with other functional devices or device components, limiting the scalable implementation of the resulted rGO powders and/or films. In this context, it remains challenging to reduce GO films and fabricate graphene-based TCFs in a viable and scalable manner, especially at conditions without any heating and transfer processes, as well as toxic agents.

In this paper, for the first time we use magnetron sputtered Sn metal layer to directly reduce pre-formed film state GO on transparent flexible substrate (PET) at room temperature. The as-prepared rGO films reach a sheet resistance of 6.7 k Ω sq⁻¹ and an optical transparency of 75 % (550 nm). The influencing factors on the reduction reaction have been systematically discussed, including the thickness of the Sn layer and the concentration of the supplementary hydrochloric acid. With further optimization, the methodology would allow for the fabrication of viable high-performance graphene-based TCFs at any substrates without any heating and transferring processes, as well as toxic agents.

Experimental

Preparation of GO

GO was prepared through a modified Hummer's method.³⁰ Typically, 10g natural flake graphite (32 mesh), 10 g sodium nitrate, and 40g potassium permanganate were mixed in 98% sulfuric acid (300 ml) for 24 hours in an ice bath. Then, the ice bath was heated at 35°C for 1 hour, after which 2L distilled water was slowly added into the suspension and stirred for 20 min before 100 ml hydrogen peroxide (3%) was added. The solution was then washed with hydrochloric acid and DI water by centrifugation for several times until the pH was about 7. The precipitates were finally redispersed in DI water to form a GO solution.



Scheme 1. Procedure of the preparation of Sn-reduced graphene film: 1) The GO film formed on PET by rod coating was covered with Sn nanoparticles via magnetron sputtering; 2) HCl solution (4M) was dropped onto the film for the reduction process; 3) Ten minutes later, the reduced film was washed by HCl solution and DI water for at least 30 times followed by a drying treatment to finally get the rGO film.

Reduction of GO film

The reduction process is shown in Scheme 1. First of all, GO solution was diluted to 1 mg/ml and then coated on PET substrate through a rod coating method.¹⁸ Then Sn layers of different thickness was magnetron sputtered onto the GO film (Other method like thermal evaporation may also be used here to uniformly cover the film with Sn metal). The film was then exposed to dilute hydrochloric acid solution (4M) for about 10 minutes to reduce the GO film. After that, the film was washed by dilute hydrochloric acid solution and DI water for several times. Finally, the rGO film was dried to remove the extra water.

Reduction of GO in solution

5ml GO solution (2 mg/ml) was added to 5ml hydrochloric acid solution (8M), and then 0.1g Sn powder was added into the solution and kept for 10min for reduction.

Characterizations

The transparency and conductivity of the rGO film were characterized by UV-vis spectrophotometer (Lambda 950) and four-point probe measurement (RTS-9) respectively. The detailed functional groups information was obtained on an X-ray Photoelectron Spectroscopy (XPS, ESCALAB250Xi). The X-ray

diffraction (XRD) measurements were executed on Rigaku D/max-2500B2 + /PCX system with Cu K α radiation. Raman spectra were collected using a Renishaw inVia Raman microscope with a laser wavelength of 514.5 nm. High resolution transmission electron microscope (HR-TEM), and selected-area electron diffraction (SAED) pattern were got from a Tecnai G2 F20 U-TWIN microscope. The morphologies of the synthesized samples were observed by a field-emission scanning electron microscope (SEM, Hitachi S4800). Thermogravimetric Analysis (TGA) data were collected on a Diamond TG/DTA. Atomic force microscopy (AFM) characterization was conducted on Nanoman II dimension 3100 operated in tapping mode.

Results and Discussion

By adjusting the coating factors (like concentration of the GO solution and the wire diameter of the rods), GO films with different thicknesses could be coated on the target substrate. Taking the GO film of 6.3nm as an example (Figure S1, †ESI), influence of Sn layer thickness on the reducing effect was explored. Figure 1a shows the square resistance of the GO film changes with the thickness of the Sn layer (Figure S1, †ESI) where the increase of the Sn thickness benefits the conductivity of the film until 8.6nm (about 1.36 times the thickness of GO film). Therefore, by choosing proper magnetron sputter factors, the performances of the film could reach the best without wasting more Sn. And as the Sn nanoparticles gradually aggregate during the sputtering process (Figure S1 b-e, †ESI) while the reducing result remains almost the same after 8.6nm, it is believed that the morphology of the Sn particles barely influence the degree of reduction. The influence of the concentration of the hydrochloric acid was also investigated (Figure S2, †ESI). It turned out that the hydrochloric acid of 4M gave the best general performance, and the probable reason will be discussed later.

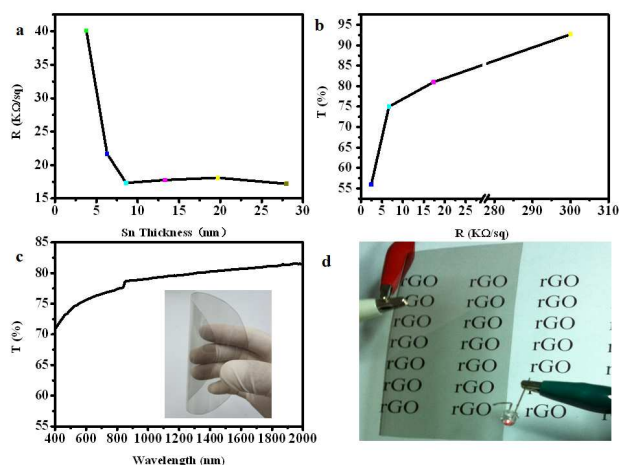


Figure 1. (a) Influence of thickness of the sputtered Sn layer to the conductivity of the rGO films (The GO films used are 6.3nm thick); (b) The transmittance at 550 nm versus sheet resistance for rGO films of different thicknesses; (c) Optical transmittance of the rGO film with an average sheet resistance of 6.7k Ω sq⁻¹ in the visible range (inset is the photo image of the flexible rGO film) and (d) photo image showing the

transparent conductive rGO film can be used in a circuit to light a red LED.

Figure 1b demonstrates the change of the transmittance along with the variation of the film resistance. The increase of the thickness of the GO film results in lower resistance and lower transmittance of the obtained rGO film at the same time. As shown in Figure 1c, the as-prepared rGO film exhibits a transmittance of 75% (550nm) and sheet resistance of $6.7 \text{ k}\Omega \text{ sq}^{-1}$, and the film is rather flexible and robust. Applied in a circuit of a red LED, the transparent rGO film can work as a conductor and light the LED with a voltage of 3V applied (Figure 1d). A comparison of the conductivity and transparency between our Sn-rGO and rGO films fabricated in other methods on flexible substrates is also made (Figure S5, †ESI). Our flexible rGO film shows a reasonable performance among these works, and those show better properties are mainly reduced by using toxic reducing agent like HI, therefore our method is rather comparative in practical applications.

To further characterize the reducing extent of the rGO film, XPS measurement was conducted on both GO and rGO films. Figure 2a is the result of general spectra for GO and rGO film, respectively. After reduction, the O1s peak dropped significantly compared with the C1s peak, indicating that a number of oxygen-containing functional groups in GO were removed. The C/O ratio

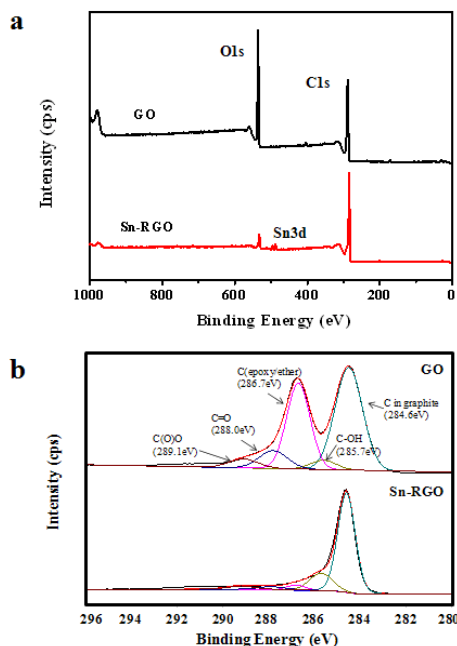


Figure 2. XPS results of (a) general spectra and (b) curve fit of C1s spectra of GO and Sn reduced GO (Sn-RGO) film, respectively.

is increased from 3.1 to 17.2 as shown in Table 1S (†ESI). There are two small peaks for Sn3d appeared in the spectrum, and the magnified figure in Figure S3 (†ESI) shows that they are centered at 487.3 eV (Sn 3d_{5/2}) and 495.8 eV (Sn 3d_{3/2}), and are assigned to a +4 formal oxidation state for the Sn element,³¹ which means Sn is oxidized to SnO₂ in this work. And to rule out the possible influence of the remaining trace amount of SnO₂ in the film to the total conductivity, the conductivity and transmittance of rGO films with different washing extent was compared (Figure S4,

†ESI). After constantly washing, there were obviously less particles on the film, while the resistance of the film remained the same ($19.6 \text{ K}\Omega/\text{sq}$), and the transmittance only increased by 0.2%, which suggested that little amount of SnO₂ particles didn't play much role in the performance of the film. The C1s spectra of GO and rGO in Figure 2b clearly show that peaks corresponding to oxygen-containing functional groups including the epoxy/ether group (286.7eV), -C=O (288.0eV) and -COO- (289.1eV) decreased sharply after reduction,³² supporting that the GO thin film was reduced by Sn metal layer by this method.

In order to better illustrate this reducing method, further characterizations such as XRD, Raman spectra, TGA, and HR-TEM were applied. As these characterizations are not available for the nano-scaled rGO film attached to substrate, rGO film was ultrasonic dispersed to prepare rGO sheet samples for these characterizations.

XRD patterns of GO and Sn-rGO are shown in Figure 3a. Due to the oxidation of pristine graphite, the (002) reflection peak shifts to lower angle ($2\theta=11.437^\circ$, d spacing= 0.773nm), compared with that at 26.6° of pristine graphite,³³ as water molecules and oxygen-containing functional groups were intercalated into the layers of the graphite. After reduction, the peak moved backwards a lot to $2\theta=23.858^\circ$, (d spacing= 0.373nm) showing that most oxygen-containing functional groups inserted were removed during the reducing process. Figure 3b presents the Raman spectra of GO and Sn-RGO. The I_D/I_G ratio of Sn-RGO slightly increased from 0.9 to 1.14 after reduction. Similar results have also been reported by other works of metal reduction on GO,^{24, 29} and this may attributed to the process of the oxygen-containing groups taking off between the GO sheets during the reduction which altered the structure, and in the mean time the random aggregation of recovered graphene structures.^{23, 34}

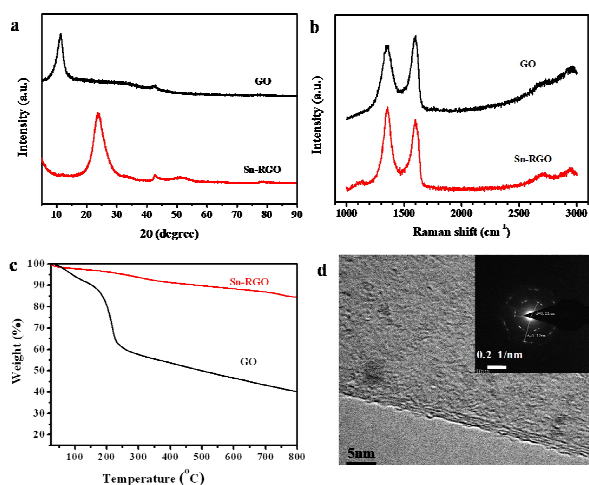


Figure 3. (a) XRD, (b) Raman, (c) TGA results of GO and Sn-RGO respectively, and (d) HR-TEM image of the Sn-RGO (inset, image of a SAED pattern).

And the intensity of 2D band of the Sn-RGO at 2680cm^{-1} is higher than GO, showing that the reduced graphene is better graphitized. The TGA plots of GO and Sn-RGO are shown in Figure 3c. Along with the temperature increased from room temperature to 800°C , the GO sample lost weight of about 60%, ascribing to the loss of water and remained oxygen-containing

groups, whereas the sample after reduction showed the loss of 15%. The comparison of the property results of our RGO film and that from other different reducing methods (mainly metal reduction) are also summarized in Table S1 (†ESI), from which we can see that our method shows a comparable reducing effect with other metal reduction works and even better than the result reported in the HI reduction work.²³ Figure 3d exhibits the HR-TEM image of the Sn-RGO, which is obviously few-layer graphene sheet as shown at the edge of the sheet. The selected area electron diffraction (SAED) patterns consist of two rings of diffraction dots show the crystalline structure of the rGO. The inner ring is generated from (1100) plane with an interplanar spacing of 0.21nm, and the outer ring is for the (2110) plane.^{23,34} The pattern is slightly diffuse because of the previous oxidation. All these data manifest that metallic Sn can be used as a reducing agent to reduce GO film to a great extent.

Compared with GO reduced in solution, GO film directly reduced in film state was more inclined to maintain the sheet morphology. As exhibited in Figure 4a, the GO sheet reduced in solution turned out to aggregate together, while the GO thin film reduced on the target substrate in Figure 4b and c appeared to be flat with only few wrinkles. It can be inferred that direct reduction of GO films, especially thin films used in our method, could be more sufficient, uniform and efficient than reduction in solution first and then fabricating films. Therefore, sputtering metal on to GO films on the target transparent substrate directly to produce rGO films combines the advantages of mild non-toxic reducing process and one-pot high-quality film fabrication on a large scale without post-transfer.

Probable mechanism of this reduction method was shown in Scheme 2. On one hand, Sn is known as an active metal with great reducing ability, just like Zn, Fe and other active metals that have been reported to reduce GO through the electron transfer from metal to the GO sheets.²⁴⁻²⁶ The reactions could be

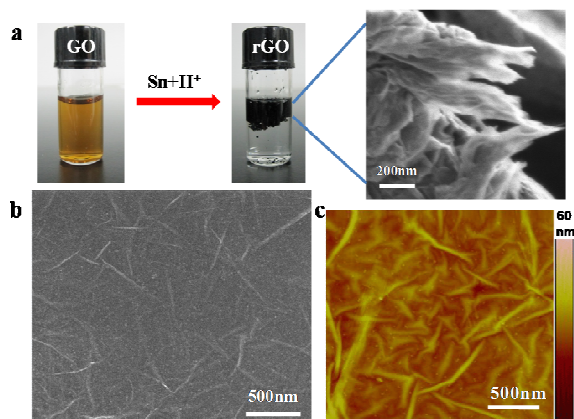
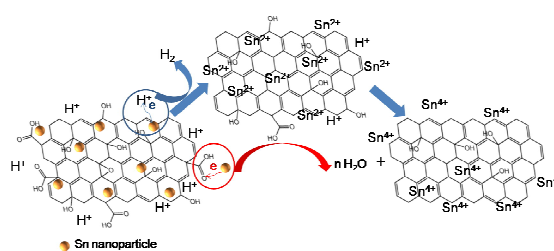


Figure 4. (a) Digital images showing the reduction process in solution, and the SEM image of the as-prepared rGO powder, (b) SEM, and (c) AFM results of Sn-RGO thin film on PET substrate.

concluded in the following equations: $M \rightarrow M^{n+} + n e^{-}$, $n H^{+} + GO + n e^{-} \rightarrow m H_2O + rGO$. Thus the high concentration of H^{+} in this system would benefit the reducing reaction. On the other hand, when exposed to H^{+} , Sn can easily be oxidized to Sn^{2+} , which is also a well-known reducing agent for GO.³⁵ In acidic environment, Sn^{2+} was inhibited to hydrolyze to sedimentation

like $Sn(OH)_2$, thus showed better reducing activity. This can also partially explain that with increasing of the hydrochloric acid concentration, the conductivity of the rGO film increased within a certain range (Figure S2, †ESI). As the reduction of GO by Sn^{2+} is quite slow at room temperature, it is reasonable to speculate that the $Sn \rightarrow Sn^{2+}$ stage plays a more important role among the two reducing stages ($Sn \rightarrow Sn^{2+}$ and $Sn^{2+} \rightarrow Sn^{4+}$). It is possible that the heat released in reaction $Sn \rightarrow Sn^{2+}$ may accelerate the process $Sn^{2+} \rightarrow Sn^{4+}$ to realize the total room temperature reduction process. Although Sn reducing GO without hydrochloric acid has also been reported recently,³⁶ it requires a necessary heating process at 85°C for 4 hours, which means the addition of hydrochloric acid can significantly enhance the efficiency of the GO reduction. Therefore, two reducing process with different electron transfer reactions may be included in the whole reaction during the same time.



Scheme 2. Probable mechanism of the reduction process.

Furthermore, this is a universal method which can be applied in other metal systems like Zn, Fe, Al, etc., yet in our experiment condition, Sn reduced GO films show better performances and higher efficiency, which may come from the two probable reducing mechanisms during the process of valence state transformation of metal Sn. This as-developed technique can also be easily employed into roll-to-roll fabrication process by modifying the metal deposition method. For instance, the Sn source could be simply deposited onto GO film by uniformly scattering Sn powder instead of magnetron sputtering onto the film.

Conclusions

In summary, a simple fast room-temperature reduction strategy for the conversion of GO films into transparent and conductive rGO films has been developed successfully by simply using metallic Sn as the reducing agent in an acid media. After a short reduction period (10 min), the prepared rGO films show a typical sheet resistance of $6.7 \text{ k}\Omega \text{ sq}^{-1}$ at a transparency of 75 %, comparable to those reduced by other toxic reducing agents. Further characterizations with TEM, XPS, XRD, Raman, and TGA indicate the high reduction efficiency of such reduction methodology. Although the electrical and optical performances of the rGO films prepared still need further improvement, this work opens a simple, economic, and environmentally friendly avenue for the scalable fabrication of graphene-based transparent conductive films because of the absence of any heating and/or transferring processes, as well as toxic agents.

Acknowledgements

The authors gratefully acknowledge the financial supports from the National Natural Science Foundation of China (Grant no. 20973044, 21173057, 21273054 and 51302045), the Ministry of Science and Technology of China (no. 2012CB933400 and 2012CB933403), the Beijing Municipal Science and Technology Commission (Z121100006812003) and the Chinese Academy of Sciences.

Notes and references

^a National Center for Nanoscience and Technology, Beiyitiao No. 11, Zhongguancun, Beijing, 100190, China. Fax: +86 10 82545578; Tel: +86 10 82545578; E-mail: zhlij@nanoctr.cn

^b University of Chinese Academy of Sciences, Beijing 100039, China

† Electronic Supplementary Information (ESI) available: Summary of the characterization results of our method and other reducing methods, AFM image of the GO film of 6.3 nm, the AFM images showing the as-sputtered Sn nanoparticle layer of different thicknesses, the influence of HCl concentration to the conductivity of the rGO film, the magnified XPS spectrum of Sn3d, the change of morphology and transmittance before and after constantly washing the film, and comparison of the conductivity and transparency between the as-prepared Sn-rGO and rGO films fabricated in other methods on flexible substrates. See DOI: 10.1039/b000000x/

These two authors contributed equally to this work.

- 25 1. X. Wang, L. J. Zhi and K. Mullen, *Nano Lett.*, 2008, 8, 323.
2. L. J. Brennan, M. T. Byrne, M. Bari and Y. K. Gun'ko, *Adv. Energy Mater.*, 2011, 1, 472.
3. S. Bae, H. Kim, Y. Lee, X. Xu, J.-S. Park, Y. Zheng, J. Balakrishnan, T. Lei, H. R. Kim, Y. I. Song, Y.-J. Kim, K. S. Kim, B. Ozyilmaz, J.-H. Ahn, B. H. Hong and S. Iijima, *Nature Nanotech.*, 2010, 5, 574.
4. B. J. Kim, C. Lee, Y. Jung, K. H. Baik, M. A. Mastro, J. K. Hite, C. R. Eddy and J. Kim, *Appl. Phys. Lett.*, 2011, 99.
5. D. S. Hecht, L. B. Hu and G. Irvin, *Adv. Mater.*, 2011, 23, 1482.
- 35 6. K. S. Novoselov, A. K. Geim, S. V. Morozov, D. Jiang, Y. Zhang, S. V. Dubonos, I. V. Grigorieva and A. A. Firsov, *Science*, 2004, 306, 666.
7. X. Huang, Z. Zeng, Z. Fan, J. Liu and H. Zhang, *Adv. Mater.*, 2012, 24, 5979.
- 40 8. W. Yuan, A. Liu, L. Huang, C. Li and G. Shi, *Adv. Mater.*, 2012, 25, 766.
9. Y. Sun, Q. Wu and G. Shi, *Energy Environ. Sci.*, 2011, 4, 1113.
10. Y. J. Gong, S. B. Yang, Z. Liu, L. L. Ma, R. Vajtai, P. M. Ajayan, *Adv. Mater.*, 2013, 25, 3979.
- 45 11. J. J. Tang, F. Di, X. Xu, Y. H. Xiao and J. F. Che, *Progress in Chem.*, 2012, 24, 501.
12. V. C. Tung, M. J. Allen, Y. Yang and R. B. Kaner, *Nature Nanotech.*, 2009, 4, 25.
13. J. P. Zhao, S. F. Pei, W. C. Ren, L. B. Gao and H. M. Cheng, *ACS Nano*, 2010, 4, 5245.
- 50 14. B.-H. Wee and J.-D. Hong, *Adv. Funct. Mater.*, 2013, 23, 4657.
15. X. Lin, J. Jia, N. Yousefi, X. Shen and J.-K. Kim, *J. Mater. Chem. C*, 2013, 1, 6869.
16. Q. Liang, S. A. Hsieh and C. P. Wong, *ChemPhysChem*, 2012, 13, 3700.
- 55 17. S.-H. Kang, T.-H. Fang and Z.-H. Hong, *J. Phys. Chem. Solids*, 2013, 74, 1783.
18. J. Wang, M. H. Liang, Y. Fang, T. F. Qiu, J. Zhang and L. J. Zhi, *Adv. Mater.*, 2012, 24, 2874.
- 60 19. H. A. Becerril, J. Mao, Z. Liu, R. M. Stoltenberg, Z. Bao and Y. Chen, *ACS Nano*, 2008, 2, 463.
20. X. Li, G. Zhang, X. Bai, X. Sun, X. Wang, E. Wang and H. Dai, *Nature Nanotech.*, 2008, 3, 538.
21. J. T. Robinson, F. K. Perkins, E. S. Snow, Z. Wei and P. E. Sheehan, *Nano Lett.*, 2008, 8, 3137.
- 65 22. G. Eda, G. Fanchini and M. Chhowalla, *Nature Nanotech.*, 2008, 3, 270.
23. I. K. Moon, J. Lee, R. S. Ruoff and H. Lee, *Nature Commun.*, 2010, 1, 73.
- 70 24. R. S. Dey, S. Hajra, R. K. Sahu, C. R. Raj and M. K. Panigrahi, *Chem. Commun.*, 2012, 48, 1787.
25. Z. J. Fan, W. Kai, J. Yan, T. Wei, L. J. Zhi, J. Feng, Y. M. Ren, L. P. Song and F. Wei, *ACS Nano*, 2011, 5, 191.
26. C. Z. Hu, X. Q. Zhai, L. L. Liu, Y. Zhao, L. Jiang and L. T. Qu, *Sci. Rep.*, 2013, 3, 2065.
- 75 27. X. G. Mei, H. Q. Zheng and J. Y. Ouyang, *J. Mater. Chem.*, 2012, 22, 9109.
28. N. H. Kim, P. Khanra, T. Kuila, D. Jung and J. H. Lee, *J. Mater. Chem. A*, 2013, 1, 11320.
- 80 29. Z. J. Fan, W. Kai, W. Wang, T. Wei, J. Yan, L. Song and B. Shao, *Carbon*, 2010, 48, 1686.
30. M. H. Liang, J. Wang, B. Luo, T. F. Qiu, L. J. Zhi, *Small*, 2012, 8, 1180.
31. F. Ye, B. Zhao, R. Ran and Z. P. Shao, *Chem. Eur. J.*, 2014, doi: 10.1002/chem.201304720.
- 85 32. S. Park, J. An, R. D. Piner, I. Jung, D. Yang, A. Velamakanni, S. T. Nguyen and R. S. Ruoff, *Chem. Mater.*, 2008, 20, 6592.
33. T. Kuila, S. Bose, P. Khanra, A. K. Mishra, N. H. Kim and J. H. Lee, *Carbon*, 2012, 50, 914.
- 90 34. X. G. Mei and J. Y. Ouyang, *Carbon*, 2011, 49, 5389.
35. Y. M. Li, X. J. Lv, J. Lu and J. H. Li, *J. Phys. Chem. C*, 2010, 114, 21770.
36. M. Chen, C. Zhang, L. Li, Y. Liu, X. Li, X. Xu, F. Xia, W. Wang and J. Gao, *ACS Appl. Mater. Interfaces*, 2013, 5, 13333.